

Do Residual Solvent Molecules Always Hinder Gas Sorption in Metal–Organic Frameworks?

Isabel Cooley and Elena Besley*



Cite This: *Chem. Mater.* 2024, 36, 219–231



Read Online

ACCESS |



Metrics & More

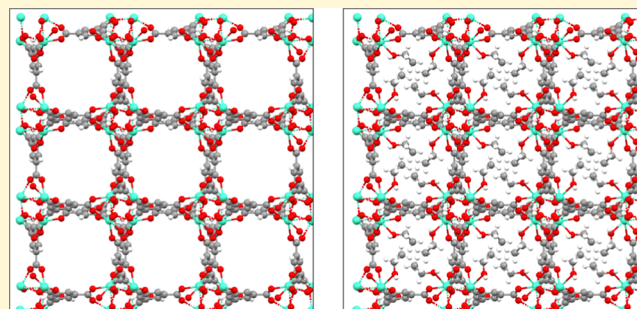


Article Recommendations



Supporting Information

ABSTRACT: The nature and magnitude of effects of residual solvent on gas uptake and selectivity in metal–organic frameworks (MOFs) have been systematically studied using high-throughput Monte Carlo simulations in the Grand Canonical ensemble. We focus on the uptake and separation of the essential CO₂ and CH₄ gases, which are pertinent to biogas upgrading and other common industrial processes and represent distinct types of interaction with the host MOF structures. We demonstrate that in circumstances where the residual solvent has a significant effect, CO₂ uptake and selectivity in a curated data set of MOFs are likely to be affected negatively by its presence, while CH₄ uptake may be affected either positively or negatively with a preference for positive effects. Both negative and positive residual solvent effects become greater at a higher pressure. Chemical, physical, and geometrical origins of the residual solvent effect have also been discussed. The relationship between various geometrical properties of MOFs and the extent of the residual solvent effect has been assessed, showing the greatest impact on MOFs with a pore diameter of around 5 Å. These results inform whether the presence of residual solvent is likely to be useful or detrimental in a MOF for a given application.



INTRODUCTION

Adsorption in porous materials provides an attractive route to efficient gas storage and separation, which are central to several industrial and environmental processes. These processes include safe and efficient delivery of next-generation methane^{1,2} and hydrogen^{3,4} fuels, capture and sequestration of greenhouse gases including CO₂,^{5,6} and separation of CO₂ and CH₄ for biogas upgrading,^{7,8} among many others. Metal–organic frameworks (MOFs) stand out as candidate materials which can be readily tuned to gas sorption requirements due to the modular nature of their assembly permitting high internal volume and surface area and a vast range of possible structures and compositions.^{9,10} However, the presence of defects or disorder in MOFs may have significant impact, either positive or negative, on gas sorption performance.¹¹

The presence of residual solvent molecules is a pertinent example of disorder, which may impact sorption properties. It is very common for the residual synthesis solvent to remain within the MOF pores (and consequently to be included in published structural information files). Experimental gas uptake studies are routinely preceded by evacuation processes aimed at solvent removal, and the effect of solvent is not regularly assessed in depth, although the impacts of incomplete or unsuccessful desolvation can be significant. Erhart et al.¹² observed this, describing the effects of the desolvation process on geometrical properties. Turning to sorption behavior, Konik et al.¹³ observed reduction in CO₂ and CH₄ uptake in two MOFs in the presence of coordinated amide solvents, noting

particular effects of the nature of the solvent. Ethiraj et al.¹⁴ examined the effect of the degree of desolvation in MOF-76-Ce on CO₂/N₂ separation. A fully desolvated form of the MOF displayed a higher total uptake, while a partially desolvated structure displayed higher selectivity, thus confirming the well-known trade-off relationship between selectivity and uptake^{15,16} and indicating that the influence of the solvent molecules can be positive or negative depending on the desired outcome.

In computational studies, evacuation is commonly performed by algorithmic removal of free and coordinating solvent molecules,^{10,17} so that solvent effects are also likely to be overlooked, though where studied their potential to impact gas sorption processes has been clear. A study by Haldoupis et al.¹⁸ involved developing optimal computational models for CO₂ adsorption in a small group of MOFs through tuning force-field parameters and adjusting the degree of solvation in the structures with water and methanol solvents. It concluded that the residual solvent molecules were likely to influence gas sorption in MOFs while commonly being overlooked. Up to

Received: August 3, 2023

Revised: December 1, 2023

Accepted: December 4, 2023

Published: December 19, 2023



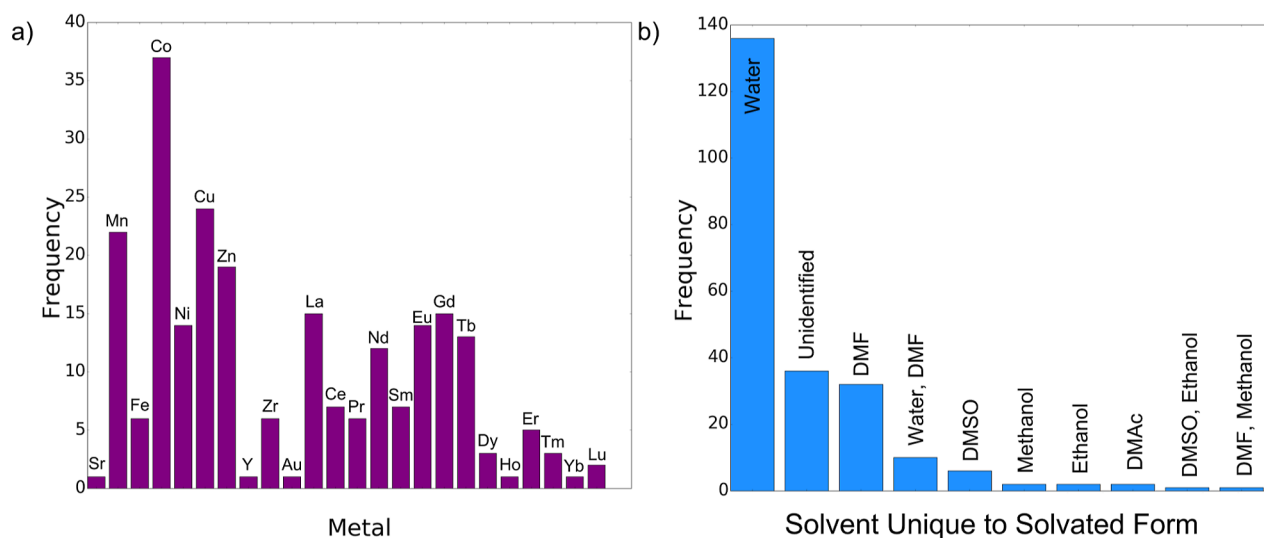


Figure 1. Histograms illustrating the abundance of metals (a) and solvents (b) in the curated data set of 225 MOFs.

around 30% of metal centers in the group of MOFs could not be detected based on surface area. The effects of the solvents on uptake events were also analyzed. While both solvents reduced total CO₂ loading due to free volume effects, the presence of water molecules led to an increase in the heat of adsorption of CO₂, while the presence of methanol led to a decrease.

In later work, Altintas et al.¹⁹ compared CH₄ and H₂ uptake at 1 bar in pairs of structures representing the same MOF but taken from two different common MOF databases.^{10,20} Different algorithms for solvent removal used in these databases account for a substantial proportion of the differences: of the 387 MOFs whose gas uptake properties differed between the two databases, the differences in 116 were defined by the presence of the bound solvent. That is, the MOF structure was given in solvated form in one database and in desolvated form in another. Comparing uptake in the solvated and desolvated forms of MOFs was not the primary purpose of the Altintas et al. study,¹⁹ but it is possible to make this comparison using their data. For example, for CH₄ uptake, higher loading in the desolvated form (solvent has a negative effect on loading) is rather common, but instances where loading is higher for the solvated form (solvent has a positive effect on loading) are also observed (Figure S1 of the Supporting Information). Similarly, while not directly considering solvent effect on uptake, Nazarian et al.²¹ made an instructive comparison of MOF structures optimized by density functional theory (DFT) and the structures taken directly from the Computation Ready Experimental (CoRE) MOF database,²⁰ where they had been deposited following crystallographic structure determination and algorithmic cleaning procedures, but not structural optimization. The results of the study by Nazarian et al.²¹ showed that MOFs from which solvent had been stripped were more likely to experience a change in sorption behavior following structural optimization, thus highlighting the geometric effects of residual solvent.

The 2019 release of the CoRE MOF database¹⁷ includes systematic consideration of solvent effects. In the database, as in this work, distinction is made between bound solvent, which is directly associated with an otherwise undercoordinated metal site, and free solvent, which interacts only weakly with

the framework. Two forms of each MOF are published: an all-solvent removed form (henceforth referred to as the desolvated form), which underwent the full desolvation procedure, and a free-solvent removed form (referred to here as the solvated form), in which the solvent identified as bound remained, and only the free solvent was stripped. The published database containing both forms was used in a high-throughput computational study of Xe and Kr uptake properties, which sought Xe-selective MOFs. It was observed that in some cases, solvent blocked favorable Xe binding sites leading to reduced uptake and selectivity. In other cases, the presence of solvent helped to provide conditions conducive to Xe uptake.¹⁷

Later, Velioglu and Keskin²² additionally measured solvent effect on processes relevant to CO₂ adsorption in a small selection of MOFs taken from the CoRE MOF database¹⁷ and Cambridge Structural Database (CSD)²³ MOF subset.¹⁰ Solvent presence was found to generally hinder the CO₂ uptake processes. This observation is of high relevance to several applications of MOFs, though it has not until now been studied on a high-throughput scale. For the CO₂ uptake process that was the focus of the study,²² positive solvent effects were not observed by Velioglu and Keskin. Removal of solvent in computational CO₂ sorption studies as a matter of course was advised. We note, however, the notable previously mentioned studies of both computational and experimental nature,^{11,14,17} which have indicated that negative effects are not exclusively observed for every process and that positive effects of solvent can also be seen.

These valuable observations of significant positive and negative impacts of solvent on gas uptake in MOFs prompt the current study, which is aimed at a greater understanding of the conditions under which elimination of residual solvent is of particular importance and those under which solvent presence should be promoted. In this work, we use high-throughput Monte Carlo simulations in the Grand Canonical ensemble (GCMC) to assess the effect of solvent on selected gas sorption processes. We focus on the uptake and separation of the essential gases CO₂ and CH₄, which also represent distinct types of interaction with the host MOF structures. Methane, the simple nonpolar hydrocarbon, is commonly modeled with no partial atomic charges, while CO₂ possesses a quadrupole moment and significant partial charges. Host structures in both

the solvated and desolvated forms are taken from the 2019 CoRE MOF database.¹⁷ We define solvent effect as the difference between the uptake in the desolvated and solvated forms of MOFs and establish relationships among solvent effect, the identity of the guest gas, and a number of geometrical properties available as part of the CoRE database. We also consider the impact of external pressure on the solvent effect.

METHODS

In any high-throughput screening study of MOFs taken directly from a database, consideration of the viability of the structures used is critical. The persistence of unfeasible structures in published databases is gaining attention as a clear limitation of the studies of this nature.^{19,22,24–27} Problems are reflected in crystallographic information files (cif) as a result of issues with experimental crystallographic structure determination and/or with computational cleaning and postprocessing of files. Common symptoms include missing hydrogen atoms, overlapping atoms, and stripping of integral parts of structures by overly zealous solvent removal algorithms. Oxidation state counting has previously been used as an efficient and effective way to detect problematic reported structures, which imply unviable or highly unlikely oxidation states.²⁶

Here, a robust data curation procedure based on a number of criteria^{8,26,28} and described in the [Supporting Information](#), was applied to the CoRE database, and as a result, several problematic structures were eliminated. Following the curation procedure, a total of 225 out of 5,928 MOFs (450 out of 11,856 structures in total, in both solvated and desolvated form) remained, which (i) possess desolvated structures different from their solvated form, (ii) were not identified as unviable structures in either form, (iii) possess geometries in both forms which indicate the possibility of admitting CO₂ and CH₄ molecules, with some leeway for flexibility,^{29,30} and (iv) had reasonable partial charges successfully assigned to their atoms using charge equilibration.³¹ Among these 225 MOFs, 24 different metal atoms make up the metal centers. In most cases, there is only one type of metal in a given MOF, but in a handful of cases, there are two. The abundance of each of the 24 metals in the data set is shown in [Figure 1a](#), indicating that the most abundant metal is Co, which appears in 37 structures, followed by Cu with 24 appearances and Mn with 22.

A MOF in the solvated subset differs from its equivalent in the desolvated subset in the presence of one or more solvent molecules. The solvent molecules that are present in the solvated subset but not in the desolvated subset were identified using a modified version of a solvent stripping python script available in the literature.¹⁰ The abundance of each of the solvents in the data set is shown in [Figure 1b](#), indicating that water is by far the most abundant solvent. The script identifies solvent molecules based on comparison of MOF fragments to a list of known solvents; however, some solvents (labeled as “Unidentified” in [Figure 1b](#)) were not present in the list utilized by the script.

With the curated data set identified, computational predictions for uptake of both CH₄ and CO₂ at 298 K in the solvated and the desolvated form of each MOF were calculated using GCMC simulations with the RASPA software package.³² With CH₄ and CO₂ uptake and separation being relevant in multiple contexts to several important industrial processes, there are sets of conditions relevant to their uptake and separation. The common pressure swing adsorption separation tends to require operation at high pressures above 10 bar,³³ while other common separation processes such as temperature swing adsorption can be carried out at lower pressures close to or below 1 bar.^{33,34} Meanwhile, the sources of CH₄ and CO₂ exist with a range of gas compositions. The biogas stream which is an important source of biomethane is composed of CH₄, CO₂, and trace gases, and the CH₄ and CO₂ compositions vary between around 50–65% and 35–50%, respectively.^{7,8,35} Gas uptake in this work was calculated at 0.1 and 1 bar for both pure single-component gases and a binary 50/50 CH₄/CO₂ gas mixture. These conditions are selected

to be appropriate for an exploratory study, which falls within relevant and readily interpretable ranges. The CO₂ selectivity, $S_{\text{CO}_2/\text{CH}_4}$, was also calculated from the binary mixture results, and is defined as

$$S_{\text{CO}_2/\text{CH}_4} = \frac{q_{\text{CO}_2} y_{\text{CH}_4}}{q_{\text{CH}_4} y_{\text{CO}_2}} \quad (1)$$

where q_i is the loading of component i in the adsorbed phase and y_i is the mole fraction of component i in the gas phase. Host MOFs were taken to be rigid, with solvent molecules treated as part of the rigid structure. Host–guest and guest–guest van der Waals and, in the case of CO₂, Coulomb interactions were computed. The van der Waals interactions were modeled using Lennard-Jones parameters taken from the Transferable Potentials for Phase Equilibria (TraPPE) formalism^{36,37} for guest gases and from the Universal Force Field (UFF)³⁸ for the host structures (including bound solvent molecules). In the high-throughput spirit of this work, standard UFF parameters were used for all of the framework atoms. This includes cases in which adjustments to parameters can improve representations, such as metal centers and, in solvated cases, for the hydrogen atoms of bound water solvent. In line with the TraPPE representations, CH₄ was represented as a single-site united atom, and CO₂ using three sites, each with a partial charge. The partial charges of framework atoms and, for solvated MOFs, also of the solvent atoms were calculated using the extended charge equilibration method, which, along with related Req methods, provides a reasonable compromise between the speed of charge evaluation and its accuracy, as shown in several high-throughput studies.^{8,15,27,39} The method was used within the RASPA software package³² and was applied with Ewald summation and a cutoff of 10^{−6}. For the Monte Carlo simulations, 15,000 equilibration cycles and 15,000 production cycles were used, with a Monte Carlo cycle consisting of N trial moves, where N is the number of molecules in the system if the system contains 20 or more molecules or 20 if the system contains fewer than 20 molecules. The trial moves translation, rotation, insertion, deletion, and, for the binary mixture case, identity change were available for selection.

The UFF is not specifically tuned to individual kinds of chemical environments and is likely to underestimate the interactions between guest gases and open metal sites (OMSs), yet it gives a physically reasonable representation of framework atoms across the periodic table, a necessary requirement for high-throughput studies. On a small computational scale, it is possible to tune the parameters for specific chemical environments, as shown successfully by Haldoupis et al.¹⁸ for a small family of M-MOF-74 structures. However, the corrected parameters fitted to systems of a particular type are unlikely to translate accurately to other systems, even to those containing the same metal center. This task would not be feasible on the scale of hundreds of MOFs used in this work. All interactions must therefore be treated with standard parameters as a compromise between the accuracy and cost. The adopted computational setup, although necessarily limited by the computational cost requirements associated with studying large numbers of MOF structures, has previously functioned well in high-throughput modeling of gas uptake in diverse MOF frameworks.^{8,17,19,27}

Similarly, development of new parameters for solvent molecules, or indeed the unique application of particular parameters to all atoms of a MOF designated as “solvent”, would be impractical for a high-throughput study. Although solvent molecules may be more labile than other MOF atoms, their movement is severely restricted, justifying their representation as rigid.¹⁸ Similar setups have been used in the previous studies which have made explicit consideration of solvent effects.^{17,22} To investigate further the nature of interactions relating to residual solvent and gas guest molecules, we carried out DFT calculations on small model systems representing solvated and desolvated metal centers (see the section “Density Functional Theory Investigation of Binding Energy to Solvated and Desolvated Metal Centers” of the [Supporting Information](#)). The DFT results provide further justification of the selected methodology.

Solvent Effects on Gas Uptake. For both the solvated and the desolvated forms of MOFs in the curated data set, uptake of CH₄ and

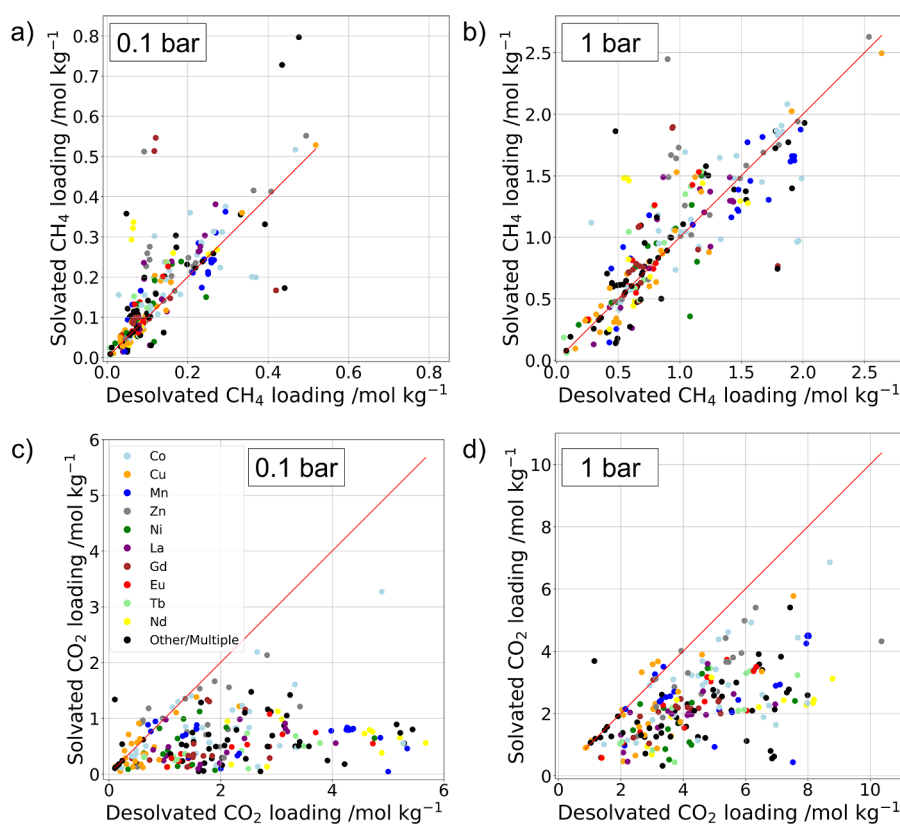


Figure 2. For 225 MOFs of the curated data set, single-component CH₄ and CO₂ loading in the solvated form against the desolvated form at 0.1 bar and at 1 bar pressure. Points are colored according to the identity of the metal center, with the ten most abundant metals in the data set colored explicitly.

CO₂ was determined in the single component and the binary mixture case at 298 K and both 0.1 and 1 bar. From the binary mixture results, the CO₂ selectivity was additionally calculated. A comparison of solvated and desolvated uptake and selectivity is aided by plotting solvated values against their desolvated counterparts. This is shown in Figure 2 (single component) and Figure 3 (binary mixture), which display a range of solvated and desolvated gas uptakes and in Figure 3 selectivity values, at both pressures. The figures show, in general, higher uptake of CO₂ than that of CH₄. The line $y = x$ is included in each plot in Figures 2 and 3 for guidance as points that lie close to the line $y = x$ correspond to MOFs which possess similar uptake or selectivity in the solvated and desolvated forms. For points that lie above the line, the solvated uptake or selectivity is higher than the desolvated uptake or selectivity, meaning that solvent has a positive effect on the measured property. For points below the line, the reverse is true: solvated uptake or selectivity is lower than the desolvated value, so solvent has a negative effect. To facilitate observation of the relationship between the atomic composition and solvent effect, points in Figures 2 and 3 are colored according to the metal center of the MOFs, including only the ten most abundant metals for clarity.

It is useful to define a measure of the effect of solvent on the considered MOF properties (CH₄ loading, CO₂ loading, and, in the case of a binary mixture, CO₂ selectivity). Throughout this work, we use the simple metric of the difference between the values in the solvated form and the values in the desolvated form of a MOF. A positive loading (or selectivity) difference corresponds to a positive effect of the solvent on loading (or selectivity). Loading and selectivity differences may be used to quantify the number of MOFs experiencing positive, negative, or little solvent effect under the conditions considered. Thresholds of loading difference slightly below and slightly above zero may be used to define the three categories of MOFs, with those falling close to zero having a small effect. The number of MOFs falling into each category using selected thresholds are summarized in Table S2 of the Supporting Information. There is a

large difference in the total magnitude of CH₄ and CO₂ loading. Therefore, different thresholds, ± 0.01 mol kg⁻¹ for CH₄ and ± 0.1 mol kg⁻¹ for CO₂, are used to distinguish the loading differences for the two gases. The threshold value of ± 5 is used for selectivity.

The definition of solvent effect based on loading difference was selected for its relevance to useful MOF applications. Alternative metrics may also be used, for example, the ratio of uptake in the solvated form to that in the desolvated form. However, at very low total uptake, the ratio may be very high even where total uptake is not usefully large, while at higher total uptake, an increase or decrease in loading that does not amount to a very significant ratio may be relevant for gas sorption applications. On the other hand, representing the threshold as the ratio of uptake in the solvated form to uptake in the desolvated form can be useful in discussions of the nature and origin of solvent effect. Plots similar to those in Figures 2 and 3, which illustrate the use of ratio metrics, along with a table equivalent to Table S2 with thresholds defined by ratio rather than difference, are given in the Supporting Information. In these plots, solvated to desolvated ratios of 0.9 and 1.1 (an effect of 10%) are used as thresholds for the loading metrics, and ratios of 0.8 and 1.2 (an effect of 20%) are used as thresholds for the selectivity metric. Possible alternatives may additionally be used that attempt to retain ratio information while avoiding exaggeration of solvent effect at very small loading. For example, a weighted loading or selectivity ratio may be employed in which the ratio is multiplied by the absolute loading.

For the single-component CH₄ gas, a significant proportion of MOF structures lie on either side of the $y = x$ line at 0.1 and 1 bar pressure, indicating that solvent may have either a positive or a negative effect on adsorption. More MOFs, however, lie above the line than below, and the points farthest from the line are on the positive side. Although both positive and negative effects are seen, the positive effect of solvent is more prevalent and, in some MOFs, can have a stronger impact than that of the negative effect. This contradicts a common and natural perception that solvent presence is

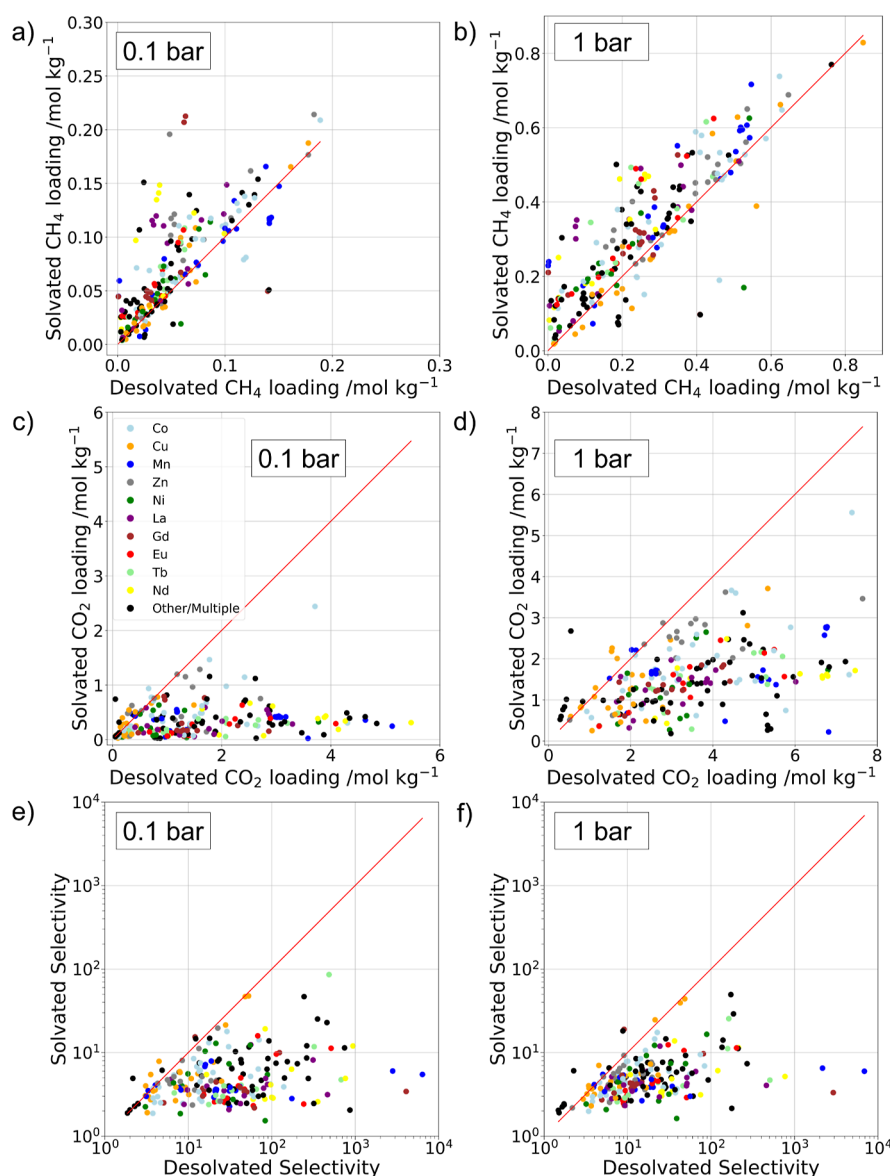


Figure 3. For 225 MOFs of the curated data set, CH₄ and CO₂ loading in the solvated form against the desolvated form for the 50/50 binary mixture at 0.1 bar and at 1 bar pressure. Points are colored according to the identity of the metal center, with the ten most abundant metals in the data set colored explicitly.

always negative, blocks binding sites, and must be minimized.^{13,22} The dominance of the positive solvent effect is slightly reduced as pressure increases, at which point the total magnitude of loading increases and the effect of volume, which is always reduced by solvent presence, thus gains significance. In the binary mixture case, although negative solvent effects on CH₄ loading remain present, the increased prevalence of positive effects is enhanced at both pressures as compared to that in the single-component case. Increased CH₄ uptake with the presence of solvent is now accompanied by reduced CO₂ uptake and, therefore, a reduction in the competition experienced by CH₄. Due to the rich diversity of MOFs, the chemical origins of both positive and negative solvent effects on CH₄ loading depend heavily on the MOF structure and may relate to a number of different factors. These include van der Waals interactions between CH₄ and the host, direct interactions with metal centers and/or ligands, and specific geometric favorability. Chemical origins of solvent effect are discussed in further detail in the section “Geometrical and Chemical Origins of Solvent Effect”.

The trends in solvent effect on CH₄ loading are fairly broad, with a range of effects observed; however, there are clear outliers, which significantly deviate from the line $y = x$. In particular, a group of three

MOFs has been noted for which in the 0.1 bar binary mixture case, the solvated loading is close to 0.2 mol kg⁻¹, but the desolvated loading is significantly less than 0.1 mol kg⁻¹. The same MOFs display qualitatively similar outlying behavior in the 0.1 bar single-component case. These MOFs have refcodes EBEXEQ, EBEXEQ01, and BUKMUQ01, and their structures are displayed in Figure 4a–c. The structures of EBEXEQ and EBEXEQ01, containing the Gd metal center and ethanol solvent, are near-identical; they represent the same MOF deposited separately in the database following separate synthesis procedures. The presence of a solvent significantly alters the nature of the space available within the pores of these MOFs. In this case, the unusually high solvated loading compared to the desolvated loading is likely related to stronger van der Waals interactions between CH₄ and the hydrocarbon part of the ethanol solvent than that between CH₄ and the Gd center. The strength of these interactions may be affected by the ethanol solvent creating a geometrically favorable environment for CH₄ to experience multiple simultaneous interactions. Meanwhile, in BUKMUQ01, the metal is Zn, and the solvent is dimethylformamide (DMF). Again, it appears that the van der Waals interactions of CH₄ with the solvent are stronger than the interactions with the exposed metal center, possibly

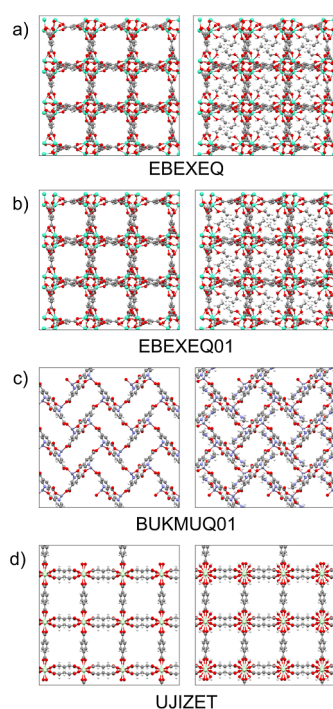


Figure 4. Desolvated (left) and solvated (right) structures of MOFs exhibiting unusual solvent behavior: (a) EBEXEQ: Gd metal center, ethanol solvent; (b) EBEXEQ01: Gd metal center, ethanol solvent; (c) BUKMUQ01: Zn metal center, DMF solvent; (d) UZIJET: Nd metal center, water solvent.

influenced by the reduction in pore size engendered by the solvent creating a geometrically more favorable environment.

The effect of solvent on the CO_2 uptake is clearly different from the CH_4 effects under each set of conditions. The majority of points fall below the $y = x$ line, indicating a negative effect of the solvent on uptake. Those which fall above the line (positive solvent effect) remain near it, and the effect is small. This is in line with the intentions to minimize solvent presence in MOFs, particularly when seeking CO_2 uptake.²² The significant increase in the negative effects of CO_2 loading compared to those of CH_4 loading is likely to be due to strong interactions of CO_2 with metal sites that are blocked by bound solvent. This reasoning implies that in only very few cases does CO_2 interact more strongly with solvent molecules than with the metal sites that they block. This is supported by the significance of the Coulomb interactions for CO_2 uptake. The partial positive charge on a metal center is generally much larger than the partial positive charges on solvent molecules, allowing the Coulomb interactions between the partially negative O atoms of CO_2 and the metal centers to be stronger than the solvent interactions. Similar to CH_4 , the specifics of the CO_2 solvent effects, their varying magnitude, and the few cases in which they are positive are governed by various factors relating to individual MOFs, which are discussed further in the section “Geometrical and Chemical Origins of Solvent Effect”.

The high prevalence of negative solvent effects on the CO_2 loading may additionally or alternatively be attributed to volume effects: the total magnitude of the CO_2 loading is in general significantly higher than that of the CH_4 loading. At a higher total loading, the available volume becomes more important, and negative solvent effects become more likely. This was probed further by normalizing solvated and desolvated loading and selectivity by accessible void fraction (VF). That is, values pertaining to solvated MOFs were divided by the accessible VF of the solvated MOF and values pertaining to desolvated MOFs were divided by the accessible VF of the desolvated MOF to give values of uptake per available volume. VFs for this purpose were taken from the CoRE MOF database.¹⁷ The VF-normalized values for desolvated loading and selectivity were then

plotted against VF-normalized values for solvated loading and selectivity and are shown in Figures S7 and S8 of the Supporting Information. If the only effect of residual solvent molecules were a volumetric one, all points in these plots would be expected to fall on the line $y = x$. Although some points do move closer to the $y = x$ line, a spread of points is still seen, implying that the solvent has energetic as well as volumetric effects on loading.

MOFs displaying an extreme solvent effect on CO_2 uptake are additionally considered. In particular, two MOFs whose desolvated loading is much higher than their solvated loading are those with refcodes BUKMUQ01 (which was also an outlier for CH_4) and UZIJET. The binary mixture CO_2 loading of BUKMUQ01 is 7.64 mol kg^{-1} in the desolvated form and 3.46 mol kg^{-1} in the solvated form. Under the same conditions, UZIJET has a loading of 7.46 mol kg^{-1} in the desolvated form and a loading of only 1.71 mol kg^{-1} in the solvated form. The structures of the two MOFs are illustrated in Figure 4c,d. In both cases, the solvent effectively blocks guest access to a metal center, which may otherwise have been a favorable interaction site, and fails to provide an equally strong interaction site to replace it.

Selectivity for CO_2 over CH_4 experiences a qualitative solvent effect similar to that of raw CO_2 loading, although the scale of the total values of selectivity is much larger (note that the selectivity plots in Figure 3 are on a logarithmic scale). The large scale of selectivity is a result of some MOFs displaying a very low CH_4 loading. The presence of solvent molecules is likely to reduce the rate of CO_2 uptake and increase CH_4 uptake, concurrently reducing the rate of CO_2 selectivity. In no case in either the desolvated or the solvated form of any MOF does selectivity fall below 1, which would indicate a reversal of selectivity, with a MOF going from CO_2 -selective to CH_4 -selective.

The atomic composition of a MOF also impacts solvent effects, and a comparison can be made among the MOFs with different metal centers. The MOFs containing the most abundant metal, cobalt, are seen to experience a range of different solvent effects, while not reaching the extremes of loading or selectivity difference. Meanwhile, copper, the second most abundant metal, appears to engender only modest solvent effects. This is in spite of the prevalence of solvated copper centers, such as copper paddlewheels, which may readily be revealed by solvent removal. These effects may be understated due to the lack of adjusted parameters in used classical force fields; however, DFT analysis included in the Supporting Information also indicates modest solvent effects for a copper center. Interestingly, in those few cases in which positive effects of CO_2 loading and selectivity are seen, copper appears frequently. The third most abundant metal, manganese, appears to follow behavior in line with the general trends of the data set: Mn-containing MOFs generally experience positive solvent effects on CH_4 loading and negative effects on CO_2 loading. Among the ten metals identified as the most frequently present in MOF structures (Figures 2 and 3), these three particularly abundant metals, along with Zn and Ni, are first-row transition metals. The remaining metal centers contain considerably more diffuse f-block elements. Although the divide between the first-row transition metal and the f-block metals is not well-defined, the f-block metals, in general, appear to display fairly strong solvent effects.

In seeking MOFs for CO_2 uptake or for selectivity of CO_2 over CH_4 , the results overall indicate that it is very rare that the presence of solvent should be encouraged. However, with the CO_2 uptake and selectivity plots including some points close to the $y = x$ line and other points very far from it comes the additional indication that in some cases, minimizing the solvent effect should be a priority, while in others, it can be overlooked without a significant effect on performance. When it comes to CH_4 capture, MOF structures exist on a significant scale in which the presence of a bound solvent ought to be encouraged in order to encourage uptake, particularly for low-pressure applications.

Relationship between Solvent Effect and Pressure. The effect engendered by the residual solvent may differ depending on external pressure, and this relationship may be examined in greater detail. We compare the solvent effect at the two pressures 0.1 and 1

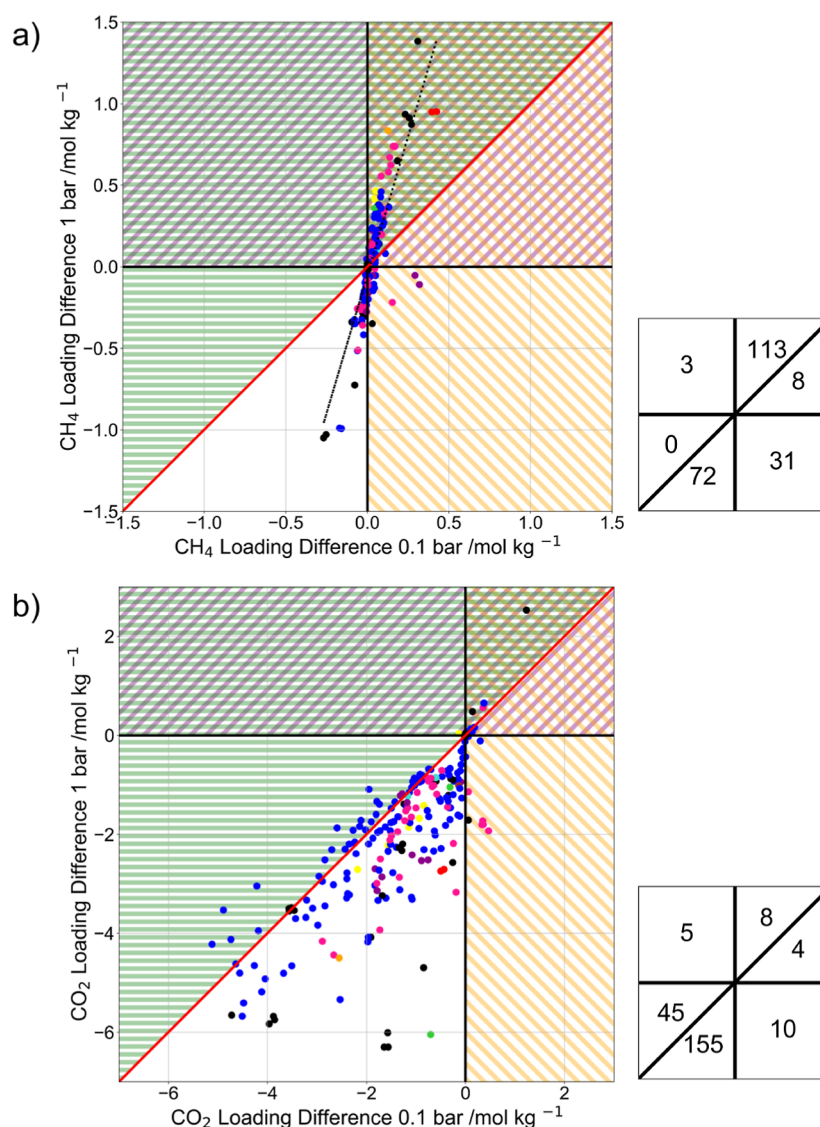


Figure 5. CH₄ (a) and CO₂ (b) loading difference at 0.1 bar against loading difference at 1 bar as calculated from single-component GCMC simulations. Loading difference is defined as the difference between the gas uptake of a MOF in the solvated and desolvated form. Lines $x = 0$ and $y = 0$ are given in black and line $y = x$ is given in red for guidance. Alongside each plot is a grid showing the number of MOFs populating the octants and quadrants formed by the guiding lines. On the CH₄ plot, a dashed regression line is shown, which has the equation $y = 3.39x - 0.051$.

bar, as measured by the loading difference and selectivity difference. In Figure 5 (single-component case) and in Figure 6 (binary mixture case), the loading difference at 0.1 bar is plotted against the loading difference at 1 bar for each of the two gases. Figure 6 additionally contains a plot of the selectivity difference at 0.1 bar against the selectivity difference at 1 bar on a symmetric log scale, as calculated from binary mixture uptake data. Points in Figures 5 and 6 are colored according to the nature of the solvent in the MOFs.

In these plots, the MOFs which lie close to the line $x = 0$ experience little solvent effect at 0.1 bar; those to the left of it experience a negative effect, i.e., presence of solvent reduces uptake or selectivity, and those to the right of it (in the orange hashed region) experience a positive effect at the same pressure. The MOFs close to the line $y = 0$ experience little effect at 1 bar; those below it experience a negative effect at 1 bar, and those above it (in the purple hashed region) experience a positive effect at 1 bar. Meanwhile, for points close to the line $y = x$, the magnitude of solvent effect as measured by difference is similar at the two pressure points; for points above the line $y = x$ (in the green hashed region) the magnitude of solvent effect is more positive at 1 bar than at 0.1 bar, and for those below it, the reverse is true. Therefore, the octant or quadrant defined by the three

lines that a point falls into describes the nature of the solvent effect on that MOF as described by the difference metric, as follows.

MOFs in the upper half of the top right quadrant (the north-northeast octant as defined by compass points, orange, purple, and green hashes) have a positive solvent effect at both pressures, and this effect is more pronounced at 1 bar than at 0.1 bar. The MOFs in the lower half of the top right quadrant (east-northeast, orange and purple hashes) have a positive solvent effect at both pressures, which is more pronounced at 0.1 bar than at 1 bar. The MOFs in the bottom right quadrant (southeast, orange hashes only) have a positive solvent effect at 0.1 bar but a negative effect at 1 bar. The MOFs in the lower half of the bottom left quadrant (south-southwest, no hashes) experience a negative solvent effect at both pressures, and the effect is more negative at 1 bar than at 0.1 bar. The MOFs in the upper half of the bottom left quadrant (west-southwest, green hashes only) also experience negative solvent effects at both pressures, but the effects are more negative at 0.1 bar than at 1 bar. The MOFs in the top left quadrant (northwest, green and purple hashes) experience a positive solvent effect at 1 bar and a negative effect at 0.1 bar. Alongside each plot in Figures 5 and 6 are grids giving the MOF population of the octants and quadrants.

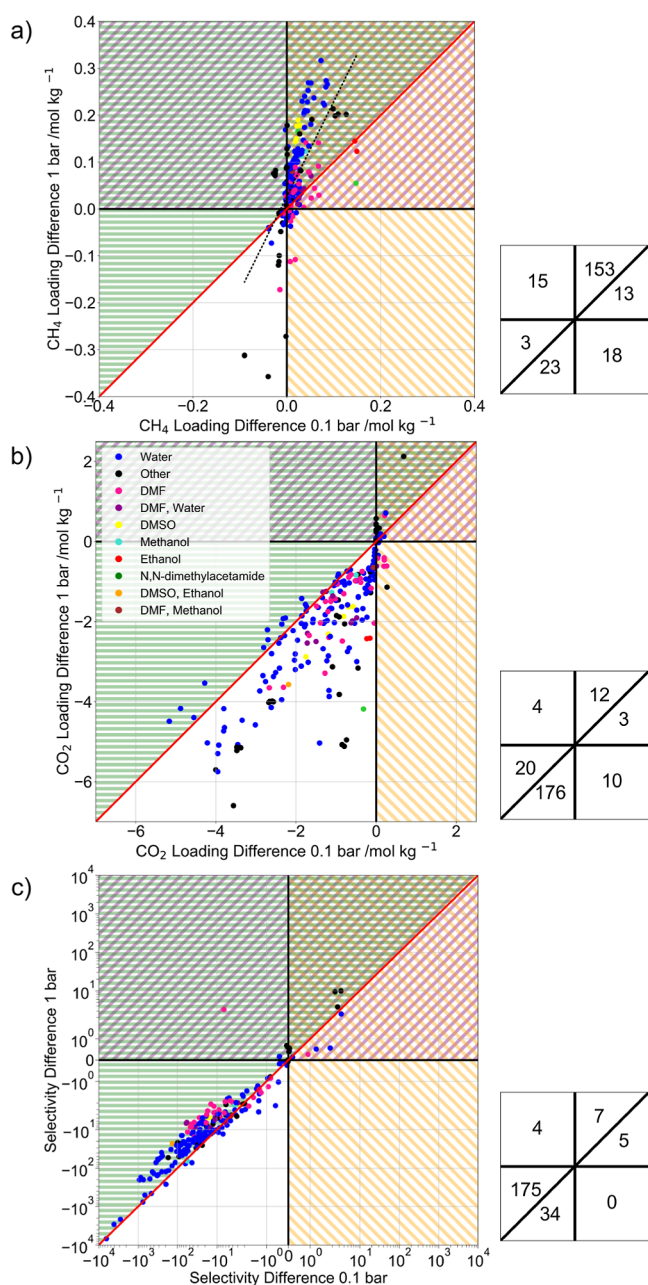


Figure 6. CH₄ (a) and CO₂ (b) loading difference at 0.1 bar against loading difference at 1 bar as well as selectivity (c) difference at 0.1 bar against selectivity difference at 1 bar, as calculated from binary mixture GCMC simulations. Loading difference is defined as the difference between gas uptake of a MOF in the solvated and desolvated forms, and selectivity difference is defined as the difference between the selectivity in the solvated form of a MOF and selectivity in the desolvate form. On the CH₄ plot, a dashed regression line is shown, which has the equation $y = 2.03x + 0.027$.

The relationship between the pressure and solvent effect on CH₄ adsorption is somewhat opposite to that for CO₂ adsorption in both the binary mixture and the single-component case. For CO₂ adsorption, the majority of points fall into the octant without hashes, which denotes a negative solvent effect at 0.1 bar and a more negative solvent effect at 1 bar. Negative solvent effects at 0.1 bar are more likely to be due to the strength of framework interactions, while the enhancement of negative effects at 1 bar is more likely related to volume availability. For CH₄, on the other hand, the most populated octant in both cases lies opposite: the north–northeast octant dashed

in purple, orange, and green, in which positive solvent effects as measured by difference are observed at both pressures, and the effects are more positive at the higher pressure. It should be noted that the behavior of CH₄ is more varying than that of CO₂, with an appreciable number of MOFs falling into the opposite south–southwest octant, particularly in the single-component plot. However, compared to CO₂, the general behavior of CH₄ molecules involves a greater likelihood of more positive interactions with solvent molecules than that with metal centers. At higher pressure, it might be expected that volume effects would countermand any increased loading, but for CH₄, the higher pressure instead facilitates an increase in the loading difference. In the single-component case, it is easily seen that the total magnitude of CH₄ loading is not sufficient for volume effects to be particularly relevant. In the binary mixture case, the presence of CO₂ dominates compared to that of CH₄, so volume effects may be expected. Indeed, the magnitude of loading difference is smaller for the binary mixture case than that for the single-component case, but the points remain in the north–northeast octant.

Interestingly, for CH₄, the MOFs fall into a reasonable approximation of a straight line, particularly in the single-component case: an approximately linear relationship exists between the solvent effect at 0.1 bar and the solvent effect at 1 bar. If the CH₄ loading difference at one pressure is known, it could be used to predict the solvent effect at the other pressure. To this end, regression lines were fit for both CH₄ loading difference cases. For the binary mixture case, the fitted line is $y = 2.03x + 0.027$ with an R^2 value of 0.43, while for the single-component case, the fitted line is $y = 3.39x - 0.051$ with a higher R^2 value of 0.71.

A general observation that stems from the analysis of all four loading plots in Figures 5 and 6 is the dominance of the northeast and southeast quadrants and within those the northeast and south–southwest octants. Few points fall into either the northwest or southeast quadrants; if the solvent has a particular effect on loading at one of the two pressures studied, that effect may be reduced or enhanced at the other pressure but is unlikely to be reversed. Once positive or negative effect at both pressures is established, an increase in pressure from 0.1 to 1 bar is likely to enhance rather than reduce the effect. That is, if the effect is negative at 0.1 bar, it is likely to be more negative at 1 bar (south–southwest octant), and if the effect is positive at 0.1 bar, it is likely to be more positive at 1 bar. From a volumetric perspective, this is intuitive for MOFs experiencing negative solvent effects. Solvent reduces the uptake in these MOFs at 0.1 bar and also reduces the available volume. At an increased pressure, the most significant expected change is a reduction in the available volume as more adsorption events occur, leading to reduction in loading. However, it might be expected that positive effects on loading would reduce as pressure increases and available volume decreases. The observed phenomenon is most likely explained by the fact that solvent effect is defined here by the difference in loading between the solvated and the desolvated form of a MOF. At a higher pressure, total loading generally increases for both forms, which causes the difference to increase, though it may decrease in relative terms.

When it comes to selectivity, the majority of MOFs fall into the west–southwest octant in Figure 6, which is on a symmetric logarithmic scale. Of those which do not fall into the west–southwest octant, the majority of MOFs lie in its neighboring south–southwest octant and are not far from the $y = x$ line which divides them. The positioning means that in most cases, the solvent has a negative impact on selectivity at both pressures, and the effect is more negative at the lower pressure. Selectivity of CO₂ over CH₄ depends on the uptake of the two gases. It relies on the magnitude of uptake, not just on uptake difference. Total selectivity tends to be higher at lower pressures, so any absolute change in selectivity is likely to be larger also, meaning a negative change in selectivity will be more negative. A potentially useful implication is that at a high enough pressure, there would be very little effect of solvent on selectivity. However, this must be balanced by the fact that at high pressure, selectivity itself can be expected to be very low, and the solvent effect on CO₂ uptake may be very negative.

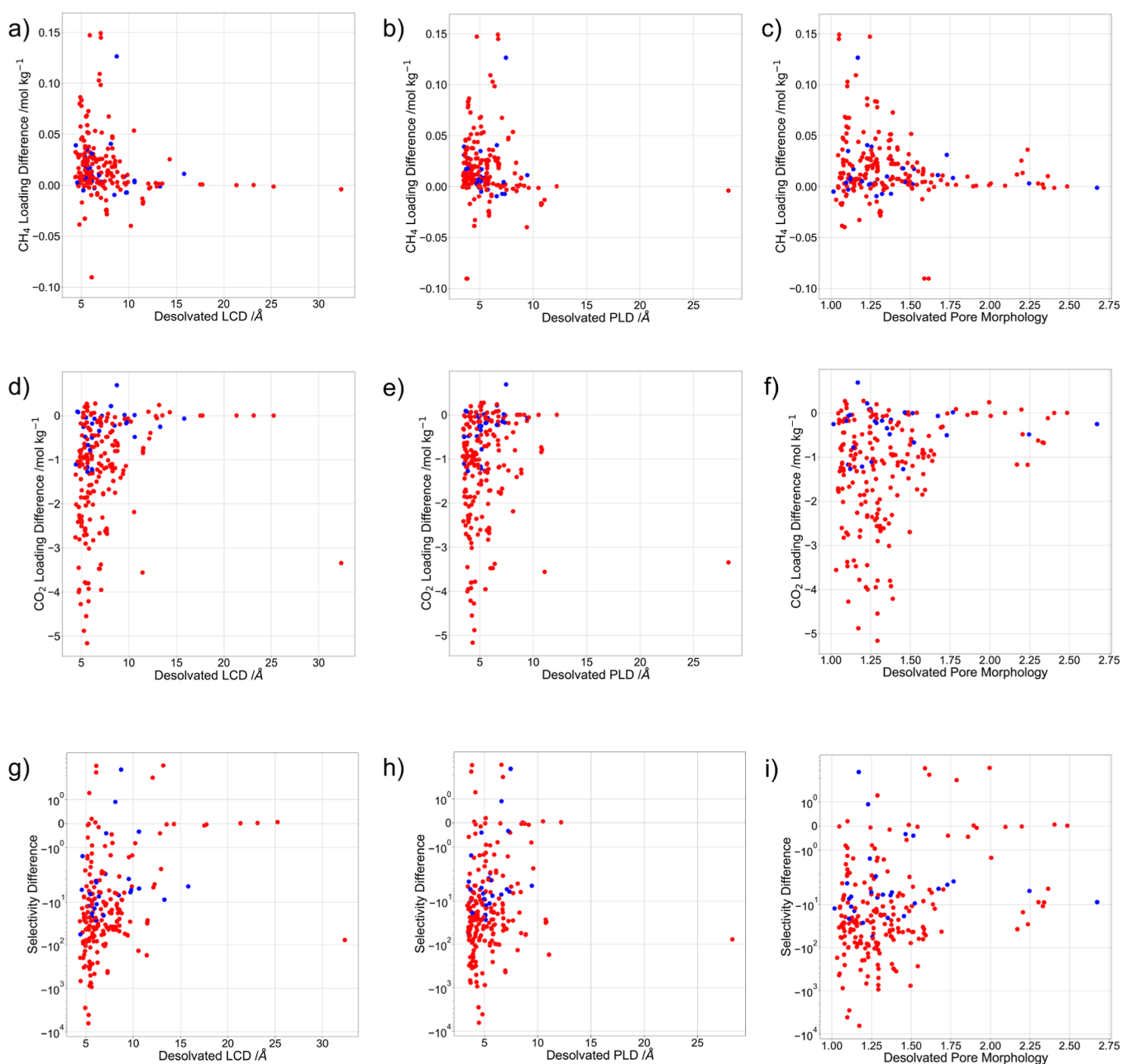


Figure 7. Desolvated PLD, LCD, and pore morphology plotted against binary mixture CH₄ uptake, CO₂ uptake, and CO₂ selectivity (symmetric log scale) at 0.1 bar. Red points: the MOF has no OMS in the solvated form. Blue points: the MOF has an OMS in the solvated form.

Similar to the thresholds defined in the previous section, the relationship between the pressure and solvent effect may be examined in the context of metrics other than loading difference, such as the ratio or a weighted ratio. With this in mind, plots of loading and selectivity ratio at 0.1 bar against the same metrics at 1 bar, similar to the difference plots given in Figures 5 and 6, are given in the Supporting Information. The effect of pressure on ratio metrics is not always the same as the effect on the difference metrics. Additionally, plots of loading and selectivity ratio weighted by total uptake in the desolvated form are given in Figures S13 and S14 of the Supporting Information. This is a further alternative, which may alleviate some of the drawbacks of the ratio metric but with which it is not straightforward to define universal solvent effect thresholds.

Geometrical and Chemical Origins of Solvent Effect. We have thus far established that CO₂ uptake and CO₂ selectivity in MOFs are likely to be affected negatively by the presence of solvent if at all, while CH₄ uptake may be affected in either direction with a

preference for positive effects. Clearly, the effect of solvent depends on more than just the guest molecule. Dependence on the features of the host MOF has been indicated by the analysis of metal centers and of outlying MOFs in the section “Solvent Effect on Gas Uptake”. Further understanding of the relationship between the solvent effect and MOF properties is desirable. We therefore compare the solvent effect metrics, uptake difference, and selectivity difference, with a selection of geometrical properties, which are available as part of the CoRE MOF database.¹⁷ We also provide additional discussion of the possible geometrical and chemical origins of the solvent effect.

The geometrical properties published in the CoRE MOF database are the largest cavity diameter (LCD), pore limiting diameter (PLD), largest free pore diameter, density, volumetric and gravimetric accessible surface area (ASA), volumetric and gravimetric non-accessible surface area (NASA), accessible volume (AV), both gravimetric and in the form of VF, and gravimetric nonaccessible volume. Further geometrical properties can be obtained from these

data. Total surface area and volume are the sums of ASA, NASA, and volume. Pore morphology, which describes whether the pores are uniform channels or have changing diameter, is given by the LCD/PLD ratio. In the CoRE database, structural information is contained for both the desolvated and solvated forms of MOFs. The database also contains information about whether an OMS is present in both forms.

We focus on data relating to structures in the desolvated form. This form is often used in computational study, and desolvated structures are readily accessible from solvated structures by use of solvent stripping scripts, which may be found in the literature.¹⁰ In many cases, the structure of the solvated form of a MOF is also available, and relationships between solvent effect and the geometry of the solvated form can also be established (see Figures S22–S29 of the Supporting Information). Complex predictive relationships between uptake and selectivity of the considered two gases and a combination of pore sizes, surface area, VF^{40–42} and, more rarely, density⁴¹ have been established previously. Gaining further understanding of the impact of these geometric properties on solvent effects is the next valuable step.

A close analysis of the relationship between geometry and solvent effect on uptake in the solvated and desolvated forms of MOFs does not yet exist in the literature, but a particular relationship appears to exist between the degree of solvation, gas uptake, and pore size and shape as defined by PLD, LCD, and pore morphology.^{12,17,19,21} Pore sizes can certainly be of critical importance for gas uptake and selectivity,^{43–46} and the finely tuned interactions that are engendered by well-selected pore sizes may be influenced by solvent presence. In Figure 7, we observe this relationship on a large scale, where PLD, LCD, and pore morphology are plotted against the uptake and selectivity difference at 0.1 bar. Equivalent plots for a 1 bar pressure are given in Figure S15 of the Supporting Information. Only plots for the binary mixture case are presented; single-component plots display similar behavior and are also shown in Figure S7 of the Supporting Information.

The existence of a relationship between the pore size and solvent effect is apparent: it is clear that smaller pores in general engender the largest solvent effect. This is particularly seen at 0.1 bar (Figure 7). While the nature of the solvent effect reverses between CO₂ and CH₄ and its magnitude reduces, the dependence of the effect on pore size is similar for the two gases. Although a small loading difference is possible over the full range of LCD and PLD, particularly large effects are for the most part only observed in MOFs with small pores. The greatest solvent effects occur in MOFs with pores of around 5 Å. The relationship between pore morphology and the solvent effect at 0.1 bar pressure follows a pattern similar to that of pore size, with the maximum solvent effect on loading occurring for small pores with the LCD/PLD ratio between 1 and 1.25 for CH₄ and between 1 and 1.5 for CO₂. There is a significantly populated tail of points corresponding to the LCD/PLD ratio greater than around 1.5 for which the solvent effect is not large, and it can be recommended that for these MOFs, significant solvent effect as measured by difference is unlikely.

When it comes to solvent effect on selectivity at 0.1 bar, the behavior is in some respects similar to the behavior of solvent effect on uptake, although the range of selectivity values, as seen in previous sections, is much larger than the range of uptake values (the selectivity plots are on a symmetric logarithmic scale). The relationships of the selectivity difference with LCD, PLD, and, in particular, pore morphology are less well-defined than those with the uptake differences. For example, there is a cluster of MOFs with LCD/PLD larger than 2 and selectivity difference between 10¹ and 10². The largest magnitude of the observed selectivity difference approaches 10⁴, but a selectivity difference of 10² is certainly significant. This cluster of points presents an obstacle to any suggestion that solvent effect can be dismissed entirely for selectivity discussions relating to MOFs with an LCD/PLD larger than a certain value. The general statement that the MOFs with a smaller LCD/PLD are more likely to have a larger absolute selectivity difference may nonetheless be made.

At a higher pressure of 1 bar (Figure S15 of the Supporting Information), the general behavior of the solvent effect with changing pore size and shape follows a similar pattern to that at 0.1 bar, although the behavior is less well-defined, and more outliers persist. In the same way as for selectivity at 0.1 bar, the poor definition hinders clear assignment of cutoffs beyond which the solvent may as a general rule be ignored, but it does not prevent general observations about the likelihood of solvent effect in MOFs of different kinds.

In Figures S16 and S17 of the Supporting Information (and Figures S18 and S19 for the single-component case), ASA (in m² g⁻¹), VF, and density of each MOF are plotted against the solvent effect metrics. At both pressures, the relationships between these properties and the solvent effect are in general less well-defined than the relationships between the pore size and shape and solvent effects. Across the range of surface areas, a very small effect of solvent on all metrics is observed at 0.1 bar (Figure S14). For CH₄ and CO₂ uptake, higher loading difference is more likely to be observed for MOFs with lower ASA, with distributions centered around 1000 m² g⁻¹. However, a very high loading can be observed outside of the general distribution. At 1 bar (Figure S15), a loose pattern of a similar nature exists between the surface area and solvent effect. At both pressures, the selectivity difference is generally large and negative at low surface area and becomes closer to zero with increasing surface area, though with many outliers. The relationships between VF and the solvent effect metrics are perhaps the most poorly defined among the geometrical properties considered at both 0.1 and 1 bar. An intermediate VF range may be seen at which particularly positive or negative CH₄ loading difference and particularly negative CO₂ loading difference are more likely to occur. However, several outliers persist for both gases. An intermediate range of densities at which a particularly positive CH₄ loading difference and particularly negative CO₂ loading difference is evident at 0.1 bar (Figure S14) but less well-defined at 1 bar (Figure S15). Furthermore, density is unusual among the geometric properties in that it correlates negatively with selectivity difference, which is the case at both pressures. Though the relationship is somewhat loose, in general, the selectivity of denser MOFs is affected more by solvent than that of the less dense MOFs.

For MOFs which possess OMSs, interaction of guests directly with these sites has commonly been seen to be an important mechanism of uptake.^{47,48} Since bound solvent is defined as the solvent interacting directly with an OMS, it may be supposed that the presence of an OMS relates strongly to the solvent effect, and indeed, the blocking of an OMS by solvent has previously been discussed in this context.¹⁷ By the definition of a bound solvent in the CoRE MOF database from which the structures were taken, desolvated MOFs are likely to possess OMSs. The majority of the solvated MOFs possess no OMS, but some possess such a site, for example, where a metal was already undercoordinated prior to desolvation or where a MOF contains more than one metal site. Examples of relevant cases are illustrated in the Supporting Information (Figure S30). We assess the relationship between the solvent effect and presence of an OMS in the solvated form of a MOF. In Figure 7, all points are colored according to whether the solvated form of the MOF possesses an OMS (blue) or not (red). An OMS is a natural location for a solvent molecule to bind, generally displaying particularly strong interactions not only with guests but also with the solvent molecules. However, as Figure 7 shows, there remains an appreciable number of MOFs in the database with an OMS in the solvated form. This illustrates the prevalence of interesting cases, such as those seen in Figure S30 of the Supporting Information, in which bound solvent is present, but metal site remains open.

For the more common and intuitive case of MOFs without an OMS in the solvated form, more negative CH₄ loading differences, selectivity differences, and in particular CO₂ loading differences are reached at both pressures than those for the interesting cases in which the solvated form does possess an OMS. Very strong negative effects are seen when desolvation uncovers an OMS in a MOF, which previously contained none: where there is no OMS in the solvated form, the presence of solvent can be instrumental in preventing the strongest interactions possible and so in negatively affecting uptake.

Positive solvent effects in MOFs with an OMS in the solvated form are more likely to be comparable to the positive solvent effects in MOFs with no OMS in the solvated form.

There are a few particularly interesting outlying points in which there is an OMS in the solvated form, and notably positive solvent effects on CO₂ uptake are seen. This includes the most positive CO₂ loading difference in the data set. Similarly, some of the most positive selectivity differences are seen in the MOFs whose solvated form contains an OMS. In these MOFs, an OMS persists despite the presence of a bound solvent in the system. Under such circumstances, a guest CO₂ molecule retains the opportunity for direct interactions with an OMS, and so the negative effect of blocking that site is avoided. This allows the solvent effect to be determined by other chemical or geometrical factors. These factors may be positive, and in such a case, positive solvent effects can be seen.

The nature of the chemical, physical, and geometrical factors, which may impact the solvent effect in such circumstances, as well as in general, must be discussed. Since diversity is a prominent characteristic of MOFs, they may be expected to display many chemical reasons for the solvent effect phenomenon. This becomes apparent considering the wide spectrum of types and magnitudes of solvent effects that have been seen to occur in this high-throughput computational study.

Most obviously, the effect of solvent on gas adsorption is likely related to the strength of interaction between a guest gas molecule and a bound solvent molecule compared to the strength of the alternative interaction between a guest gas molecule and the metal atom, which the solvent blocks. In many cases, it appears to be the dominant factor. For CO₂, these interactions are modeled using a Coulomb and a van der Waals contribution, while for CH₄, only the van der Waals contribution is considered.^{36,37} Metal atoms are typically assigned high positive partial charges. This means that the Coulomb contribution from direct interactions between the partial negative charges on the O of CO₂ and the metal centers will be particularly high, and blocking these centers with solvent is likely to reduce uptake. As CH₄ is modeled as a nonpolar molecule without partial charges, Coulomb interactions, which have a high likelihood of engendering negative solvent effects, are not relevant to CH₄ loading where van der Waals interactions dominate. These do not rely on the significant partial charges present on metal atoms, and van der Waals interactions between CH₄ and the solvent may be stronger than those between CH₄ and the metal center. Hence, positive effects could be seen. This was observed for EBEXEQ, EBEXEQ01, and BUKMUQ01 MOF structures and described in the section “Solvent Effect on Gas Uptake”.

Although metal centers are a common and intuitive binding site for guest molecules, more general effects of the MOF structure must also be considered. The binding sites in MOFs for various guest gases,⁴³ including CO₂ and CH₄,⁴⁹ can be complex; ligands, as well as metal centers, can be instrumental to guest binding. This can be particularly true for nonpolar guests. It is also more likely to occur for molecular guests of larger size since a possible reason for the phenomenon is relative inaccessibility of the metal center. CH₄ is therefore more likely to be affected by these considerations, but they may also be relevant to CO₂. In cases where primary binding sites occur on ligands rather than on metal centers, it may be expected that only small, volumetric solvent effects on loading would be seen. There are other ways that the solvent may affect loading. If a solvent molecule is large enough or the metal center is close to a ligand binding site, the solvent may sterically block the site and negatively affect loading. However, a solvent molecule in the vicinity of a ligand binding site may alternatively enhance binding to that site and positively affect loading by providing an additional van der Waals (or Coulombic) interaction for a guest molecule occupying the site. Similarly, if the metal center is inaccessible to a guest but accessible to a smaller solvent molecule, the solvent molecule, once bound, may provide an additional favorable binding site for the guest gas that was not present in the desolvated form of the MOF and so engender positive effects on loading.

Finally, bound solvent molecules have the potential to impact the geometry of a MOF and thereby influence solvent effects. It is well-

known that the close geometrical compatibility between a guest gas molecule and a MOF framework can be instrumental in facilitating adsorption and selectivity. MOF pore sizes can be carefully tuned to different uptake scenarios and cause favorable interactions on multiple sites at once. However, solvent molecules may alter pore size and disturb the tuning, which can have a negative effect on uptake by reducing geometrical compatibility or a positive effect by increasing compatibility. In summary, the observed solvent effects can have a variety of underpinning causes including a combination of volumetric and geometric effects and strong interactions with metal centers and ligands.

CONCLUSIONS

In this study, the effect on the adsorption of residual solvent in MOF pores has been systematically assessed with the aid of GCMC calculations. This solvent may persist in MOF pores following its use in synthesis and may have a significant effect on gas uptake and selectivity if it does. To further understand this phenomenon, uptake and selectivity of CH₄ and CO₂ have been calculated for MOFs with and without bound solvent in their pores. The difference in uptake and selectivity afforded by the solvent has been used to draw conclusions about the nature and magnitude of solvent effects in situations relevant to common industrial processes.

Both positive and negative effects of the solvent have been observed. Where solvent does have a significant effect on CO₂ uptake, it is seen that the effect is almost exclusively negative under various conditions and tends to be more negative at higher pressure. Uptake of CH₄ is more likely to be positively affected by solvent presence, although it can be negatively affected also. Where it is positively affected, the effect tends to be more positive at higher pressure.

The physical, chemical, and geometrical origins of solvent effect have also been discussed, and the relationship between the geometrical properties of MOFs and the extent of solvent effect has been assessed. A relationship between the pore size and shape and solvent effect is seen in which smaller pores are more likely to be affected strongly by solvent presence than the larger pores. Other geometrical properties, surface area, volume, and density, display similar but looser relationships with solvent effect. All of the individual geometrical relationships are complex. Alone, they cannot be used to make confident predictions for a given MOF, but they can be used to state general guidelines about the likelihood of significant solvent effects in different types of geometry.

The results of this work may be used to provide guidance about whether and to what extent the presence of a solvent is likely to be useful or detrimental in a MOF for a given application. They may also be used to inform future studies attempting to establish further statistical relationships between MOF properties and solvent effects or pursuing detailed modeling of solvent effects in individual structures.

ASSOCIATED CONTENT

Supporting Information

The Supporting Information is available free of charge at <https://pubs.acs.org/doi/10.1021/acs.chemmater.3c01940>.

Reference methane data; curation of MOF structures; DFT investigation of binding energy to solvated and desolvated metal centers; solvent effects in the curated MOF data set; relationship between solvent effect and pressure: alternative metrics; and examples of OMS situations (PDF)

AUTHOR INFORMATION

Corresponding Author

Elena Besley – School of Chemistry, University of Nottingham, Nottingham NG7 2RD, U.K.; orcid.org/0000-0002-9910-7603; Email: elena.besley@nottingham.ac.uk

Author

Isabel Cooley – School of Chemistry, University of Nottingham, Nottingham NG7 2RD, U.K.

Complete contact information is available at:

<https://pubs.acs.org/10.1021/acs.chemmater.3c01940>

Notes

The authors declare no competing financial interest.

ACKNOWLEDGMENTS

E.B. acknowledges a Royal Society Wolfson Fellowship for financial support.

REFERENCES

- (1) Peng, Y.; Krungleviciute, V.; Eryazici, I.; Hupp, J. T.; Farha, O. K.; Yildirim, T. Methane Storage in Metal-Organic Frameworks: Current Records, Surprise Findings, and Challenges. *J. Am. Chem. Soc.* **2013**, *135*, 11887–11894.
- (2) He, Y.; Zhou, W.; Qian, G.; Chen, B. Methane Storage in Metal-Organic Frameworks. *Chem. Soc. Rev.* **2014**, *43*, 5657–5678.
- (3) Murray, L. J.; Dinca, M.; Long, J. R. Hydrogen Storage in Metal-Organic Frameworks. *Chem. Soc. Rev.* **2009**, *38*, 1294–1314.
- (4) Chen, B.; Ockwig, N. W.; Millward, A. R.; Contreras, D. S.; Yaghi, O. M. High H₂ Adsorption in a Microporous Metal-Organic Framework with Open Metal Sites. *Angew. Chem., Int. Ed.* **2005**, *44*, 4745–4749.
- (5) Ding, M.; Flaig, R. W.; Jiang, H.-L.; Yaghi, O. M. Carbon Capture and Conversion using Metal-Organic Frameworks and MOF-Based Materials. *Chem. Soc. Rev.* **2019**, *48*, 2783–2828.
- (6) Millward, A. R.; Yaghi, O. M. Metal-Organic Frameworks with Exceptionally High Capacity for Storage of Carbon Dioxide at Room Temperature. *J. Am. Chem. Soc.* **2005**, *127*, 17998–17999.
- (7) Chen, X. Y.; Vinh-Thang, H.; Ramirez, A. A.; Rodrigue, D.; Kaliaguine, S. Membrane Gas Separation Technologies for Biogas Upgrading. *RSC Adv.* **2015**, *5*, 24399–24448.
- (8) Glover, J.; Besley, E. A High-Throughput Screening of Metal-Organic Framework Based Membranes for Biogas Upgrading. *Faraday Discuss.* **2021**, *231*, 235–257.
- (9) Wilmer, C. E.; Leaf, M.; Lee, C. Y.; Farha, O. K.; Hauser, B. G.; Hupp, J. T.; Snurr, R. Q. Large-Scale Screening of Hypothetical Metal-Organic Frameworks. *Nat. Chem.* **2012**, *4*, 83–89.
- (10) Moghadam, P. Z.; Li, A.; Wiggin, S. B.; Tao, A.; Maloney, A. G. P.; Wood, P. A.; Ward, S. C.; Fairen-Jimenez, D. Development of a Cambridge Structural Database Subset: A Collection of Metal-Organic Frameworks for Past, Present, and Future. *Chem. Mater.* **2017**, *29*, 2618–2625.
- (11) Iacomini, P.; Formalik, F.; Marreiros, J.; Shang, J.; Rogacka, J.; Mohmeyer, A.; Behrens, P.; Ameloot, R.; Kuchta, B.; Llewellyn, P. L. Role of Structural Defects in the Adsorption and Separation of C₃ Hydrocarbons in Zr-Fumarate-MOF (MOF-801). *Chem. Mater.* **2019**, *31*, 8413–8423.
- (12) Erhart, O.; Georgiev, P. A.; Krautscheid, H. Desolvation Process in the Flexible Metal-Organic Framework [Cu(Me-4py-trzia)], Adsorption of Dihydrogen and Related Structure Responses. *CrystEngComm* **2019**, *21*, 6523–6535.
- (13) Konik, P. A.; Berdonosova, E. A.; Savvotin, I. M.; Klyamkin, S. N. The Influence of Amide Solvents on Gas Sorption Properties of Metal-Organic Frameworks MIL-101 and ZIF-8. *Microporous Mesoporous Mater.* **2019**, *277*, 132–135.
- (14) Ethiraj, J.; Bonino, F.; Vitillo, J. G.; Lomachenko, K. A.; Lamberti, C.; Reinsch, H.; Lillerud, K. P.; Bordiga, S. Solvent-Driven Gate Opening in MOF-76-Ce: Effect on CO₂ Adsorption. *ChemSusChem* **2016**, *9*, 713–719.
- (15) Qiao, Z.; Xu, Q.; Jiang, J. Computational Screening of Hydrophobic Metal-Organic Frameworks for the Separation of H₂S and CO₂ From Natural Gas. *J. Mater. Chem. A* **2018**, *6*, 18898–18905.
- (16) Shah, M. S.; Tsapatsis, M.; Siepmann, J. I. Identifying Optimal Zeolitic Sorbents for Sweetening of Highly Sour Natural Gas. *Angew. Chem., Int. Ed.* **2016**, *55*, 5938–5942.
- (17) Chung, Y. G.; Haldoupis, E.; Bucior, B. J.; Haranczyk, M.; Lee, S.; Zhang, H.; Vogiatzis, K. D.; Milisavljevic, M.; Ling, S.; Camp, J. S.; Slater, B.; Siepmann, J. I.; Sholl, D. S.; Snurr, R. Q. Advances, Updates, and Analytics for the Computation Ready, Experimental Metal Organic Framework Database: CoRE MOF 2019. *J. Chem. Eng. Data* **2019**, *64*, 5985–5998.
- (18) Haldoupis, E.; Borycz, J.; Shi, H.; Vogiatzis, K. D.; Bai, P.; Queen, W. L.; Gagliardi, L.; Siepmann, J. I. Ab initio derived force fields for predicting CO₂ adsorption and accessibility of metal sites in the metal-organic frameworks M-MOF-74 (M = Mn, Co, Ni, Cu). *J. Phys. Chem. C* **2015**, *119*, 16058–16071.
- (19) Altintas, C.; Avci, G.; Daglar, H.; Nemati Vesali Azar, A.; Erucar, I.; Velioglu, S.; Keskin, S.; Keskin, S. An Extensive Comparative Analysis of Two MOF Databases: High-Throughput Screening of Computation-Ready MOFs for CH₄ and H₂ adsorption. *J. Mater. Chem. A* **2019**, *7*, 9593–9608.
- (20) Chung, Y. G.; Camp, J.; Haranczyk, M.; Sikora, B. J.; Bury, W.; Krungleviciute, V.; Yildirim, T.; Farha, O. K.; Sholl, D. S.; Snurr, R. Q. Computation-Ready, Experimental Metal-Organic Frameworks: A Tool to Enable High-Throughput Screening of Nanoporous Crystals. *Chem. Mater.* **2014**, *26*, 6185–6192.
- (21) Nazarian, D.; Camp, J. S.; Chung, Y. G.; Snurr, R. Q.; Sholl, D. S. Large-Scale Refinement of Metal-Organic Framework Structures Using Density Functional Theory. *Chem. Mater.* **2017**, *29*, 2521–2528.
- (22) Velioglu, S.; Keskin, S. Revealing the Effect of Structure Curations on the Simulated CO₂ Separation Performances of MOFs. *Mater. Adv.* **2020**, *1*, 341–353.
- (23) Groom, C. R.; Bruno, I. J.; Lightfoot, M. P.; Ward, S. C. The Cambridge Structural Database. *Acta Crystallogr.* **2016**, *72*, 171–179.
- (24) Chen, T.; Manz, T. A. Identifying Misbonded Atoms in the 2019 CoRE Metal-Organic Framework Database. *RSC Adv.* **2020**, *10*, 26944–26951.
- (25) Chen, T.; Manz, T. A. A Collection of Forcefield Precursors for Metal-Organic Frameworks. *RSC Adv.* **2019**, *9*, 36492–36507.
- (26) Burner, J.; Luo, J.; White, A.; Mirmiran, A.; Kwon, O.; Boyd, P. G.; Maley, S.; Gibaldi, M.; Simrod, S.; Ogden, V.; Woo, T. K. ARC-MOF: A Diverse Database of Metal-Organic Frameworks with DFT-Derived Partial Atomic Charges and Descriptors for Machine Learning. *Chem. Mater.* **2023**, *35*, 900–916.
- (27) Sturluson, A.; Huynh, M. T.; Kaija, A. R.; Laird, C.; Yoon, S.; Hou, F.; Feng, Z.; Wilmer, C. E.; Colón, Y. J.; Chung, Y. G.; Siderius, D. W.; Simon, C. M. The Role of Molecular Modelling and Simulation in the Discovery and Deployment of Metal-Organic Frameworks for Gas Storage and Separation. *Mol. Simul.* **2019**, *45*, 1082–1121.
- (28) Ongari, D.; Boyd, P. G.; Kadioglu, O.; Mace, A. K.; Keskin, S.; Smit, B. Evaluating Charge Equilibration Methods To Generate Electrostatic Fields in Nanoporous Materials. *J. Chem. Theory Comput.* **2019**, *15*, 382–401.
- (29) Schneemann, A.; Bon, V.; Schwedler, I.; Senkovska, I.; Kaskel, S.; Fischer, R. A. Flexible metal-organic frameworks. *Chem. Soc. Rev.* **2014**, *43*, 6062–6096.
- (30) Chen, L.; Reiss, P. S.; Chong, S. Y.; Holden, D.; Jelfs, K. E.; Hasell, T.; Little, M. A.; Kewley, A.; Briggs, M. E.; Stephenson, A.; Thomas, K. M.; Armstrong, J. A.; Bell, J.; Busto, J.; Noel, R.; Liu, J.; Strachan, D. M.; Thallapally, P. K.; Cooper, A. I. Separation of Rare Gases and Chiral Molecules by Selective Binding in Porous Organic Cages. *Nat. Mater.* **2014**, *13*, 954–960.

- (31) Wilmer, C. E.; Kim, K. C.; Snurr, R. Q. An Extended Charge Equilibration Method. *J. Phys. Chem. Lett.* **2012**, *3*, 2506–2511.
- (32) Dubbeldam, D.; Calero, S.; Ellis, D. E.; Snurr, R. Q. RASPA: Molecular Simulation Software for Adsorption and Diffusion in Flexible Nanoporous Materials. *Mol. Simul.* **2016**, *42*, 81–101.
- (33) Shang, J.; Hanif, A.; Li, G.; Xiao, G.; Liu, J. Z.; Xiao, P.; Webley, P. A. Separation of CO₂ and CH₄ by Pressure Swing Adsorption Using a Molecular Trapdoor Chabazite Adsorbent for Natural Gas Purification. *Ind. Eng. Chem. Res.* **2020**, *59*, 7857–7865.
- (34) Jiang, L.; Wang, R. Q.; Gonzalez-Diaz, A.; Smallbone, A.; Lamidi, R. O.; Roskilly, A. P. Comparative Analysis on Temperature Swing Adsorption Cycle for Carbon Capture by Using Internal Heat/Mass Recovery. *Appl. Therm. Eng.* **2020**, *169*, 114973.
- (35) Huertas, J. I.; Giraldo, N.; Izquierdo, S. *Mass Transfer in Chemical Engineering Processes*; InTech, 2010; pp 133–135.
- (36) Martin, M. G.; Siepmann, J. I. Transferable Potentials for Phase Equilibria. 1. United-Atom Description of n-Alkanes. *J. Phys. Chem. B* **1998**, *102*, 2569–2577.
- (37) Potoff, J. J.; Siepmann, J. I. Vapor-Liquid Equilibria of Mixtures Containing Alkanes, Carbon Dioxide, and Nitrogen. *AIChE J.* **2001**, *47*, 1676–1682.
- (38) Rappe, A. K.; Casewit, C. J.; Colwell, K. S.; Goddard, W. A.; Skiff, W. M. UFF, a Full Periodic Table Force Field for Molecular Mechanics and Molecular Dynamics Simulations. *J. Am. Chem. Soc.* **1992**, *114*, 10024–10035.
- (39) Li, W.; Rao, Z.; Chung, Y. G.; Li, S. The Role of Partial Atomic Charge Assignment Methods on the Computational Screening of Metal-Organic Frameworks for CO₂ Capture under Humid Conditions. *ChemistrySelect* **2017**, *2*, 9458–9465.
- (40) Aghaji, M. Z.; Fernandez, M.; Boyd, P. G.; Daff, T. D.; Woo, T. K. Quantitative Structure–Property Relationship Models for Recognizing Metal Organic Frameworks (MOFs) with High CO₂ Working Capacity and CO₂/CH₄ Selectivity for Methane Purification. *Eur. J. Inorg. Chem.* **2016**, 4505–4511.
- (41) Fernandez, M.; Woo, T. K.; Wilmer, C. E.; Snurr, R. Q. Large-Scale Quantitative Structure-Property Relationship (QSPR) Analysis of Methane Storage in Metal-Organic Frameworks. *J. Phys. Chem. Lett.* **2013**, *117*, 7681–7689.
- (42) Fernandez, M.; Boyd, P. G.; Daff, T. D.; Aghaji, M. Z.; Woo, T. K. Rapid and Accurate Machine Learning Recognition of High Performing Metal Organic Frameworks for CO₂ Capture. *J. Phys. Chem. Lett.* **2014**, *5*, 3056–3060.
- (43) Simon, C. M.; Mercado, R.; Schnell, S. K.; Smit, B.; Haranczyk, M. What Are the Best Materials To Separate a Xenon/Krypton Mixture? *Chem. Mater.* **2015**, *27*, 4459–4475.
- (44) Sikora, B. J.; Wilmer, C. E.; Greenfield, M. L.; Snurr, R. Q. Thermodynamic Analysis of Xe/Kr Selectivity in over 137,000 Hypothetical Metal-Organic Frameworks. *Chem. Sci.* **2012**, *3*, 2217–2223.
- (45) Presser, V.; McDonough, J.; Yeon, S. H.; Gogotsi, Y. Effect of Pore Size on Carbon Dioxide Sorption by Carbide Derived Carbon. *Energy Environ. Sci.* **2011**, *4*, 3059–3066.
- (46) Mahmoud, E. Evolution of the Design of CH₄ Adsorbents. *Surfaces* **2020**, *3*, 433–466.
- (47) Fischer, M.; Hoffmann, F.; Fröba, M. New Microporous Materials for Acetylene Storage and C₂H₂/CO₂ Separation: Insights from Molecular Simulations. *ChemPhysChem* **2010**, *11*, 2220–2229.
- (48) Mohamed, M. H.; Yang, Y.; Li, L.; Zhang, S.; Ruffley, J. P.; Jarvi, A. G.; Saxena, S.; Vesper, G.; Johnson, J. K.; Rosi, N. L. Designing Open Metal Sites in Metal - Organic Frameworks for Paraffin/Olefin Separations. *J. Am. Chem. Soc.* **2019**, *141*, 13003–13007.
- (49) Benson, O.; da Silva, I.; Argent, S. P.; Cabot, R.; Savage, M.; Godfrey, H. G.; Yan, Y.; Parker, S. F.; Manuel, P.; Lennox, M. J.; Mitra, T.; Easun, T. L.; Lewis, W.; Blake, A. J.; Besley, E.; Yang, S.; Schröder, M. Amides Do Not Always Work: Observation of Guest Binding in an Amide-Functionalized Porous Metal–Organic Framework. *J. Am. Chem. Soc.* **2016**, *138*, 14828–14831.